Presented at 11th International Workshop on Breast Imaging, Pennsylvania (8-11 July 2012)
doi: 10.1007/978-3-642-31271-7_44

A Modelling Framework for Evaluation of 2D-Mammography and Breast Tomosynthesis systems.

Premkumar Elangovan[1], Alistair Mackenzie[2,3], Oliver Diaz[1], Alaleh Rashidnasab[1], David R. Dance[2,3], Kenneth C. Young[2,3], Lucy M. Warren[2,3], Eman Shaheen[4] , Hilde Bosmans[4], Predrag R. Bakic[5], and Kevin Wells[1]

[1]Centre for Vision, Speech and Signal processing, University of Surrey, Guildford, GU2 7XH, UK
[2]NCCPM, Royal Surrey County Hospital, Guildford, Surrey, GU2 7XX, UK
[3]Department of Physics, University of Surrey, Guildford, GU2 7XH, UK
[4]Department of Radiology, University Hospitals Leuven, Herestraat 49, 3000 Leuven, Belgium
[5]Department of Radiology, University of Pennsylvania, Philadelphia, PA 19104, USA
p.elangovan@surrey.ac.uk

Abstract. Planar 2D X-ray mammography is the most common screening technique used for breast cancer detection. Digital breast tomosynthesis (DBT) is a new and emerging technology that overcomes some of the limitations of conventional planar imaging. However, it is important to understand the impact of these two modalities on cancer detection rates and patient recall. Since it is difficult to adequately evaluate different modalities clinically, a collection of modeling tools is introduced in this paper that can be used to emulate the image acquisition process for both modalities. In this paper, we discuss image simulation chains that can be used for the evaluation of 2D-mammography and DBT systems in terms of both technical factors and observer studies.

Keywords: Digital breast tomosynthesis, 2D-mammography, modeling, simulation.

1 Introduction

Breast cancer is one of the major causes of mortality in women in North America and Western Europe [1]. As a result breast screening programmes have been introduced in many western countries [2]. Mammography is the accepted radiological imaging technique for this purpose that uses low energy X-rays to image internal structures of the breast. An ideal mammogram is one in which the normal breast tissues such as adipose and glandular tissues can be differentiated from lesions and calcifications that are the signatures of malignancy. In reality, the quality and interpretation of a mammogram are affected by factors, such as overlapping tissues, dose, image processing and system characteristics.

One of the most promising advances in the field of breast cancer imaging is digital breast tomosynthesis (DBT) - a technique that uses low dose projections acquired at different angles to construct tomographic planes parallel to the detector. A commonly used reconstruction algorithm is the filtered back projection [3] because of its rapid execution time, but the 3D reconstruction is not perfect due to the limited number of projections. Further, tomosynthesis also suffers from similar quality degradation issues as a conventional 2D mammogram. However, tomosynthesis is considered to be a step forward in the field of breast imaging because clinical studies [4] have shown that a better visualization of lesions and calcifications can be achieved by blurring the appearance of overlapping tissues in the image.

It is important to understand the impact of tomosynthesis on the detection and recall rates of the patients who are invited for screening before considering this new modality for routine breast screening. Performing a comparison clinically is particularly time consuming and expensive, and some evaluations could be conducted more easily using mathematical modeling tools.

In this paper, we address this issue by introducing a modeling framework which includes a collection of simulation tools that can be used to represent the image acquisition process for planar mammography and for DBT. With this framework, it is possible to perform a comparison of 2D mammography and DBT systems. A brief introduction to the modeling tools is given in Section 2 and some selected simulation results are presented in Section 3.

2 Materials and Methods

For the initial development of the model, we have simulated 2D and DBT systems manufactured by Hologic (Bedford, Massachusetts, USA), as such systems are available in our centre, though the methodology can in principle be applied to any mammographic imaging system. The Hologic Selenia Dimensions 3D system is equipped with an a-Se (amorphous selenium) detector with a pixel pitch of 70 μm. The system can operate in both 2D mammography and 3D tomosynthesis mode. The dimensions of the detector are 24x29 cm^2 and an anti-scatter grid can be positioned above the detector to reduce the scatter during the acquisition of 2D mammograms. When operating in tomosynthesis mode, the X-ray source moves continuously over the angular range +7.5º to -7.5º, and 15 projections are acquired during this process. The center of rotation of the X-ray tube is directly above the a-Se layer of the detector. After acquisition, the pixels are resampled to a pitch of 140μm. No anti-scatter grid is used during tomosynthesis acquisition and the projections are reconstructed into breast planes of 1mm thickness.

Figure 1 shows the flowcharts of the modeling framework. A brief description of each module is given in section 2.1 followed by the methodology in section 2.2.

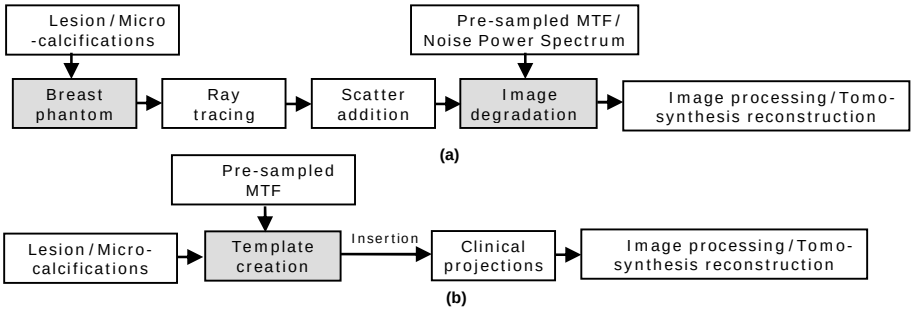

Fig. 1. Flowcharts illustrating the simulation chains described in Section 2.2, (a) using breast phantom and (b) using clinical projections

2.1 Modeling Tools

Breast phantom. We used the software breast phantoms developed by Bakic *et al* [5]. These phantoms include all the primary breast tissues such as adipose tissue, fibroglandular tissue, Cooper's ligaments and skin. The simulation parameters of the breast model can be modified to account for variations in the breast anatomy such as thickness and glandularity.

Lesion simulation model. We used lesion simulation tool proposed by Rashidnasab *et al* [6-7], which uses fractal growth methods such as DLA (diffusion limited aggregation) and Random walk, to grow lesions in a 3D space. The model parameters can be varied to control the simulated mass structure and size. The DLA approach generates lesions that have porous interior and irregular boundaries, whereas Random walk approach generates lesions with relatively symmetric appearance. The dataset used here included both benign and malignant simulated masses. The methods had been validated by means of observer studies and found to provide realistic lesions.

Micro-calcification simulation model. We used the validated built 3D models of micro-calcification clusters developed by Shaheen *et al* [8]. The authors scanned biopsy specimen containing micro-calcifications using a micro-CT scanner, and subsequently segmented the calcifications from the background using thresholding techniques. The dataset used here included mainly malignant micro-calcification clusters, and their realistic appearance had been validated by means of observer studies.

Ray tracing tool. We used a ray tracing tool based on the Siddon algorithm [9] which computes the path traveled by an X-ray photon inside a voxelized phantom. The tool stores an individual record of each unique tissue and its path length traversed by a ray. This information was used to create a primary image using Beer's law and attenuation coefficients [10] corresponding to the appropriate mammographic X-ray spectrum [11].

Scatter addition tool. We used the scatter kernels proposed by Diaz *et al* [12], as a replacement for Monte Carlo simulations, to model scatter in mammography and tomosynthesis systems. Scatter kernels, whose coefficients depend on the breast thickness, glandularity and air gap at each pixel point, were convolved with the primary image to generate the scatter map. The model also accounted for the scatter from the compression paddle and the incident angle of the x-ray photons.

Conversion of image quality tool. We used the methods of Mackenzie *et al* [13], which use measurements of the signal transfer properties, pre-sampled MTF (Modulation Transfer Function) and NPS (Noise Power Spectrum) performed on a tomosynthesis imaging system, to adapt the image quality of acquired images or simulated images. These measurements were used to blur the projection images and then add noise corresponding to a specific detector pixel size and specific exposure parameters respectively. The image was first scaled such that the pixel value was equivalent to the detector air kerma. The blurring process involved convolving a pre-sampled MTF and movement blur of the system being modeled with the projection images as shown in equation 1, where I_0 is the projection image and $H(u,v)$ is MTF of the system.

$$I_{blur} = FFT^{-1}\{\, FFT\{I_0(x,y)\} \cdot MTF(u,v) \,\} \tag{1}$$

Subsequently, addition of noise to the blurred images involved creation of three flat field images, one for each major noise source (structure, electronic, quantum) from the NPS coefficients calculated for a detector air kerma of 1 μGy. The noise coefficients were then converted into real images (I_e: electronic noise, I_q: quantum noise and I_s: structure noise) equivalent to the noise at 1 μGy. The noise was added as shown in equation 2 using the knowledge of the dose to the detector and its response to electronic, quantum and structure noise.

$$I_{blur+noise} = I_e(x,y) + I_q(x,y)\sqrt{I_{blur}(x,y)} + I_s(x,y)I_{blur}(x,y) + I_{blur}(x,y) \tag{2}$$

Image processing tool. The Selenia V4.7.3 FFDM image processing package was used to convert the raw image thus calculated into an image for presentation to the radiologists.

Tomosynthesis reconstruction tool. The Hologic reconstruction software was used to reconstruct the tomographic breast image planes from the projection images.

2.2 Methodology

An initial experiment was conducted whereby the masses [6-7] and micro-calcifications [8] were inserted into the breast phantom [5] by replacing the tissue voxels with lesion/micro-calcification voxels at appropriate locations. One mammogram and 15 tomosynthesis primary projections were acquired using the ray tracing tool [9], Beer's law and attenuation coefficients [10] corresponding to the appropriate X-ray spectrum [11], at different angles in accord with the Hologic specification. The information such as thickness, glandularity, and air gap that is

required for the selection of appropriate scatter kernels [12] was extracted from the ray tracing results and fed into the tool, for addition of scatter to the primary images. Using the MTF and noise model [13], a system MTF was applied to the projections corresponding to the detector and system, and noise was added to the projections corresponding to a specific dose. The effect of projection angle on the pre-sampled MTF and NPS were also taken into account. Each 2D-mammogram was post-processed using the Selenia V4.7.3 FFDM image processing package. The remaining 15 tomosynthesis projections were processed using the Hologic tomosynthesis reconstruction tool.

In a second experiment, the aforementioned methodology was adapted as follows: instead of a phantom, lesions and micro calcifications were inserted into clinical 2D-mammograms and individual tomosynthesis projections. The method of insertion into 2D-mammogram was adopted from Rashidnasab *et al* [6-7], and the method of insertion into tomosynthesis projections was adopted from Shaheen *et al* [8]. A series of templates were created from the projections of the lesion or micro-calcifications. At the desired location of insertion, each pixel in the template was multiplied by the corresponding pixel in each of the raw projection images. Prior to insertion, the scatter was removed from the insertion site, and after modification of the transmission factors by multiplication of the template, the scatter was added back.

Further, the model was validated by simulating a phantom that is used for routine quality control of mammography equipments, and comparing the modeled outcome with the ground truth data. The phantom comprised a 4.5cm polymethyl methacrylate (PMMA) block resting on the breast support, and an aluminum foil of dimension 10x10x0.2 mm^3 placed 1 cm above the breast support. Since this setup is representative of a 5.3cm breast, which is typically used for exposure measurements, an airgap of 8mm is allowed between the compression paddle and the top of the PMMA block for geometrical and exposure consistency. Other modeling parameters included: 23μGy average detector entrance air kerma per projection; tungsten target and aluminum filter (0.7mm) at 31kVp; and SPR (scatter to primary ratio) of 0.5. The average detector entrance air kerma for the modeled projections, for the sake of noise addition, was estimated from the known signal transfer properties of the detector and the average pixel value in the actual projections. Both actual and modeled projections were reconstructed using the same version of the reconstruction software for consistency.

3 Results

Figure 2 shows the actual and modeled projections along with the corresponding reconstructed tomographic planes. CNR (contrast to noise ratio) measurements were performed on the in focus plane at which the aluminum foil was located. The CNR measurement for the actual and modeled planes had a reasonably good agreement; the percentage error was approximately 15%. Discrepancy in the CNR may have been due to error in the detector air kerma approximation and also possibly due to reconstruction artifacts. Other contributing factors could have been the effect of phase lag and blurring due to finite size of the focal spot, which were not accounted for.

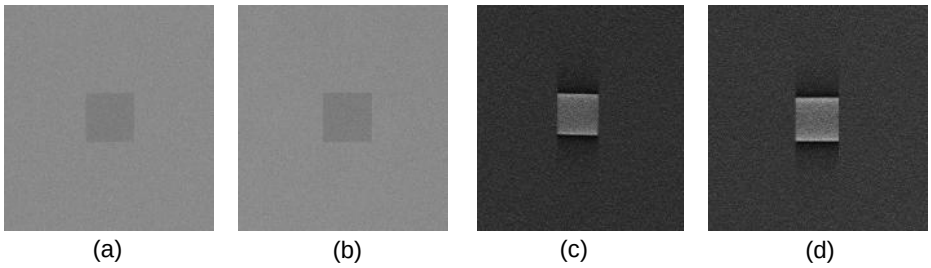

Fig. 2. (a) Actual projection; (b) modeled projection; (c) actual plane; (d) modeled plane.

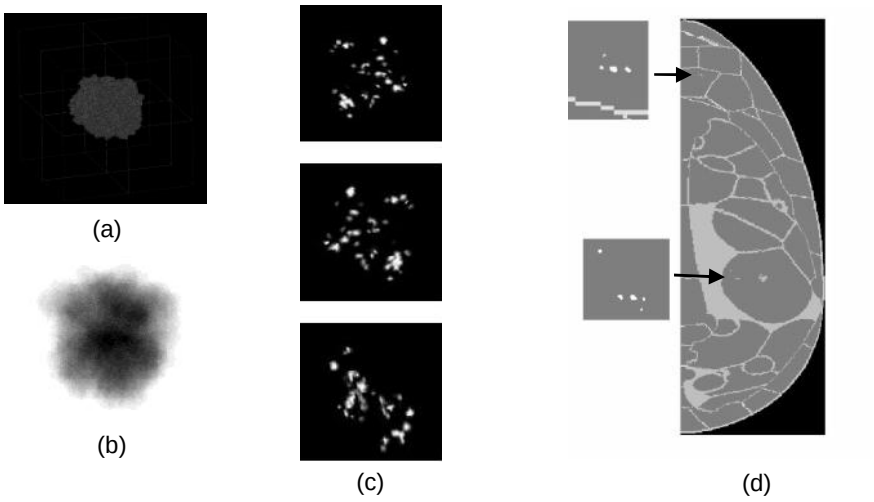

Fig. 3. (a) Simulated lesion rendered in 3D; (b) 2D projection of the lesion; (c) micro-calcifications; (d) breast phantom with micro-calcifications inserted into an adipose region to highlight visibility.

Figure 3 shows the results of insertion of a micro-calcification cluster (cluster size: 5mmx4mmx4mm; >30 calcifications) into the breast phantom (thickness: 65mm; dense tissue: 25%) alongside an example of a simulated mass and micro-calcification cluster. Figure 4 shows the results of insertion of a relatively large (~12mm) conspicuous lesion (method: random walk; fractal dimension:2.82) into clinical projections followed by the application of the reconstruction software. Figure 5 shows a processed 2D mammogram and reconstructed tomographic plane of a breast with a small (~5mm) subtle simulated lesion (method: DLA; fractal dimension: 2.54). It is obvious from Figure 5 that there are significant variations in the lesion appearance between both modalities. Impact of this distinction on the cancer detection can be determined by conducting further studies using the proposed framework.

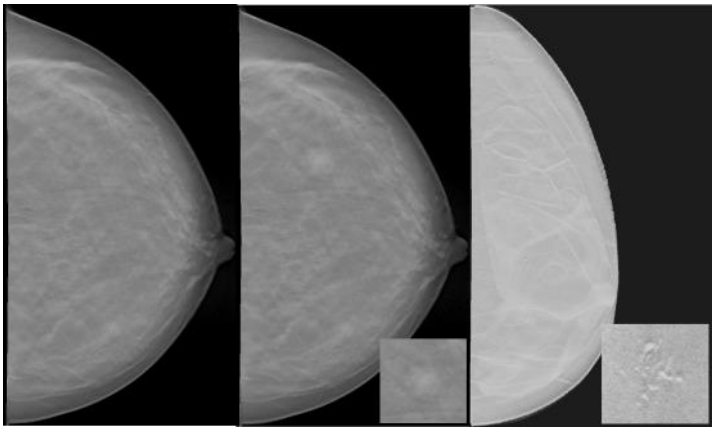

Fig. 4. Reconstructed tomographic breast plane from (a) clinical projections prior to insertion of a simulated lesion; (b) clinical projections after insertion of a 12mm obvious simulated lesion; (c) breast phantom projections with inserted micro-calcifications.

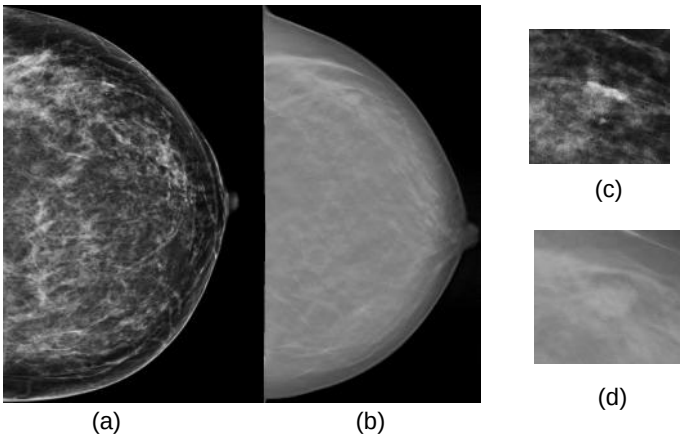

Fig. 5. (a) Processed 2D mammogram of a breast with a 5mm subtle simulated lesion; (b) reconstructed tomographic plane of the same breast; (c-d) thumbnail insets showing inserted regions in detail.

4 Discussions and Conclusions

A modeling framework to simulate 2D-mammography and digital breast tomosynthesis systems has been proposed to allow comparative studies. The simulation chain using breast phantoms demonstrated its use for studying the impact of technical factors on the image formation and image quality. The other simulation

chain using clinical images demonstrated that this is useful for conducting observer performance studies to investigate the detectability of lesions in 2D and DBT.

Acknowledgements. This work is part of the OPTIMAM project and is supported by Cancer Research-UK & EPSRC Cancer Imaging Programme in Surrey, in association with the MRC and Department of Health (England). We would like to thank Celia Strudley at NCCPM, RSCH for her timely help and support for this work. We are grateful for the help and support of staff from the Jarvis Breast Screening Unit, Guildford. Also, we would like to thank Hologic for providing us with the reconstruction tool and image processing software.

References

1. Parkin, D.M. and Fernandez L.M.G.: Use of statistics to assess the global burden of breast cancer. The Breast Journal 12, 70-80 (2006).
2. NHS Breast Screening Programme, Annual Review 2009, http://www.cancerscreening.nhs.uk/breastscreen/publications.
3. Mertelmeier, T., Orman, J., Haerer, W. and Dudam, M.K.: Optimizing filtered backprojection reconstruction for a breast tomosynthesis prototype device. Proc. SPIE 6142, 61420F1-61420F12 (2006).
4. Teertstra, H.J., Loo, H.J., Van den Bosch, M.A, Van Tinteren, H., Rutgers, E.J., Muller, S.H. and Gilhuijs, K.S.: Breast tomosynthesis in clinical practice: initial results. Eur Radiol. 20, 16-24 (2010).
5. Bakic, R.B., Zhang, C. and Maidment, A.D.A.: Development and characterization of an anthropomorphic breast software phantom based upon region-growing algorithm. Med.Phys 38. 3165-3176 (2011).
6. Rashidnasab, A., Elangovan, P., Dance, D.R., Young, K.C., Diaz, O. and Wells, K.: Modeling realistic breast lesions using diffusion limited aggregation. Proc.SPIE 8313, 83134L(2012).
7. Rashidnasab, A., Elangovan, P., Young, K.C., Dance, D.R., Yip, M., and Wells, K.: Realistic simulation of breast mass appearance using random walk. Proc.SPIE 8313, 83130L (2012).
8. Shaheen, E., Ongeval, C.V., Zanca, F., Cockmartin, L., Marshall, N., Jacobs, J., Young, K.C., Dance, D.R., and Bosmans, H.: The simulation of 3D microcalcification clusters in 2D digital mammography and breast tomosynthesis. Med.Phys. 38, 6659 (2011).
9. Siddon, R.L.; "Fast calculation of the exact radiological path for a three-dimensional CT array. Med.Phys.12, 252-255 (1985).
10. Berger, M.J., Hubbell, J.H., Seltzer, S.M., Chang, J., Coursey, J.S., Sukumar, R. and Zucker, D.S.: XCOM: Photon cross sections database. NIST Standard Reference Database 8, 87-3597 (1998).
11. Boone, J.M., Fewell, T.R. and Jennings, R.J.: Molybdenum, Rhodium and Tungsten anode spectral models using interpolating polynomials with application to mammography. Med.Phys. 24, 1863-1874 (1997).
12. Diaz, O., Dance, D.R., Young, K.C., Elangovan, P., Bakic, P.R. and Wells, K.: A fast scatter field estimator for digital breast tomosynthesis. Proc.SPIE 8313. 831305 (2012).
13. Mackenzie, A., Workman, A., Dance, D.R., Yip, M., Wells, K. and Young, K.C.: Development and validation of a method for converting images to appear with noise and sharpness characteristics of a different detector and X-ray system. Med.Phys. 39, In press (2012).